UNIVERSITY OF CALIFORNIA,

IRVINE

Characterizing lateral diffusion of EGFR using advanced fluorescence spatial correlation functions

THESIS

submitted in partial satisfaction of the requirements

for the degree of

MASTER OF SCIENCE

in Biomedical Engineering

by

Jim Jacob Kalassery

Thesis Committee:

Associate Professor Michelle Digman, Chair
Professor Enrico Gratton
Professor Geoffrey Abbott

2016

TABLE OF CONTENTS

LIST OF FIGURES

Page

ACKNOWLEDGMENTS

I would like to express my grateful appreciation to my thesis adviser Prof. Michelle Digman, my valuable committee members, Prof. Enrico Gratton , and Prof. Geoffrey Abbott. It was entirely an honor to be part of LFD, and I am extremely thankful to Dr. Digman and Dr. Gratton for providing me this opportunity and all helping me walk all the baby steps in path of learning use of fluorescence dynamics in biomedical engineering.

I would like to thank Dr.Jenu Varghese Chacko, Dr.Leonel Malacrida, Dr.Hongtao Chen and Milka Stakic for providing me with necessary training, guidance to the fulfillment of my project. I would also like to thank my beloved lab mates : Jenu Chacko, Andrew Trinh, Michael Murata, Emma Mah, Ning Ma and Sara Sameni for making every day in lab enjoyable and memorable.

ABSTRACT OF THE THESIS

Characterizing lateral diffusion of EGFR using advanced fluorescence spatial correlation functions

By

Jim Kalassery

Master of Science in Biomedical Engineering

University of California, Irvine, 2016

Associate Professor Michelle Digman, Chair

Epidermal growth factor receptor (EGFR) has various functionalities in the cell cycle and also plays an important role in cellular transport. EGFR is found to be localized on the cell membrane before its activation. Although, there are numerous studies that focus on the transport and signaling mechanism of EGFR mediated cellular transport, only few studies have been done in the area characterizing its lateral diffusion. In our work, we focus on characterizing EGFR lateral diffusion prior to and after activation of the receptor by epidermal growth factor using Total Internal Fluorescence Reflection Microscopy (TIRF). TIRF microscopy uses camera based data collection and novel pixel based correlation methods enable us to analyze and study a diffusing population. One can record whole cell, and analyze and decipher the predominant diffusion mechanisms presented in the cell using the techniques like pair-correlation function, image mean square displacement, number and brightness, etc. This thesis presents the very first trial to correlate EGFR movement within a cell using these techniques.

CHAPTER 1: Background

1.1 EGFR receptor functionality and actin cytoskeleton relationship

The plasma membrane is a highly packed moiety comprising of many surface proteins including receptors and ion channels. The question about the organization of these proteins in the plasma membrane is important in the understanding of receptor triggering and downstream signaling. The organization of receptors on the membrane was previously considered to be random distributed on the cell surface. [1] However, it is now well accepted that the membrane and proteins alike are compartmentalized giving rise to topological protein organization (from monomers to high-order oligomers) on the plasma membrane. Among these proteins is the epidermal growth factor receptor (EGFR). It plays a significant role in cell growth, differentiation, motility and proliferation. [2-4]. It is well studied that upon activation, EGFR, which predominantly exists in monomeric form prior to activation, exists as a homodimer (Figure. 1) [5]. But some studies have pointed out that EGFR may also exist in higher order oligomeric forms once activated [6]. Recent research has concluded that this receptor behavior is highly dependent on factors such as cell type, receptor expression, temperature, experimental conditions. [7] But it is evident that clusters with varying number of receptors coexist.

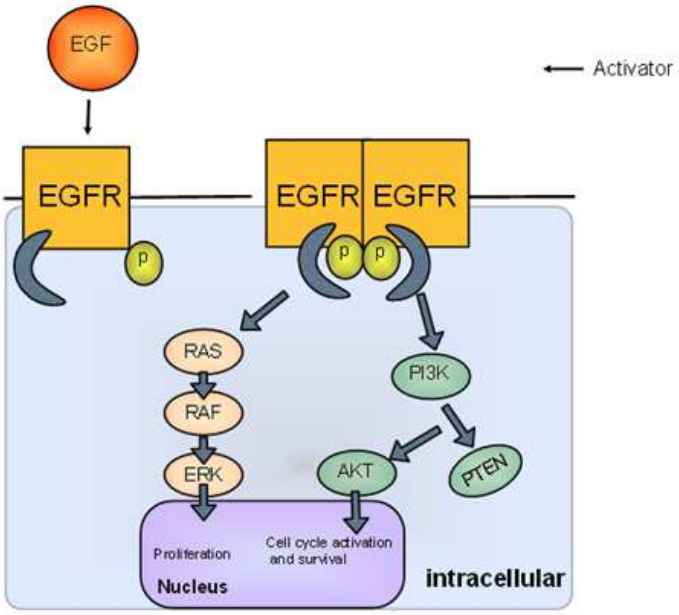

Figure 1: EGF activation of EGFR, showing dimerization and intracellular signaling resulting in various cell functions

Actin cytoskeleton has been implicated to have a role to play in lateral diffusion of EGFR clusters [8-10]. A recent study, focused on two particular elements of the cytoskeleton, actin filaments and microtubules, and their involvement in the diffusion of EGFR clusters [11]. Single particle tracking (SPT) method was used to track the fluorescently tagged EGFR clusters and mean square displacement (MSD) technique was used to study different modes of diffusion of individual EGFR clusters. Two important results from this study was, that the disruption of actin filaments increase the mobility of EGFR clusters, while the disruption of microtubules decreases the overall mobility [11]. One possible avenue by which disruption of microtubules has impacted the diffusivity is by the redistribution of the caveolae dependent proteins and the formation of signaling complexes. [11-12] But this relationship is not fully understood and the impact of caveolae on diffusivity on EGFR clusters is thus a very important element that need to

be understood for a wider understanding of the functionality of the receptor. In our research, we study this relationship and try to verify the impact of caveolae on overall diffusivity of the receptor.

1.2 Caveolin and Epidermal Growth Factor interaction and localization

Caveolin is an integral transmembrane protein and plays a significant role in interactions of integrin receptors with cytoskeleton associated and signaling molecules. [13] Compartmentalization of EGFR into caveolae helps with preventing EGFR degradation and also enables intracellular EGFR signaling. [14] This process has implications in nuclear transport of EGFR to assist with DNA repair. [15-16]

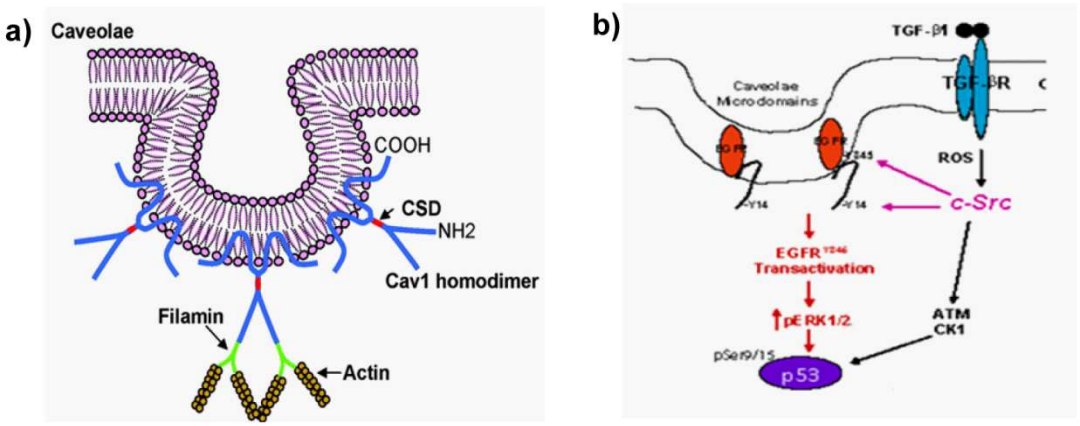

Figure 2: a) Caveolin structure, anchored by actin cytoskeleton [17] b) shows signaling pathway involving Src signaling and EGFR transactivation resulting in downstream p53 activation

EGFR is localized on the membrane and often found to be concentrated in caveolae rich regions (Figure.2). EGFR moves out of the caveolae, if it is activated by ligand induced binding [18]; specifically, for the purposes of our experiment, this is our expected

response to the addition of EGF. This movement is independent of clathrin coated pits [19]. While, there have been studies showing post stimulation by EGF, and in some cases EGFR moves out of caveolin pits and into transmembrane [20], the modes of diffusion have not been characterized. In our work, we aim to study the underlying diffusion mechanism that enables the transport post stimulation by EGF.

1.3 Methods to study EGFR-Caveolin diffusivity on cell membrane

Recent studies on EGFR activation has emerged focused on characterizing the ligand activation of EGFR by observing for its dimerization using different analytical methods to confirm the accepted mode of activation [21-23]. In this study, we plan to prove the increase in dimeric EGFR by using Number and Brightness (N&B) analysis technique. Characterizing the diffusion of the receptor across the membrane, upon activation is the stated aim of this study, for this purpose, we use Image Mean square displacement (IMSD) technique to study lateral diffusion after addition of EGFR ligand, EGF.

Single particle Tracking (SPT) has been predominantly used as a means to understand clustering of EGFR as well as a means to understand the diffusion characteristics [24]. SPT is an important tool in observing direct protein dynamics and interactions. However, the number of molecules that can be observed in a time period is limited, rendering the technique unreliable in studying rapid phenomena for a large number of events [25]. IMSD use an entire image for the analysis thereby allowing us to observe the whole cellular interaction and the particulars of receptor activity across the whole membrane [26].

CHAPTER 2: Analysis Techniques

2.1 Diffusion role on cell membrane

Our work focuses on the lateral diffusion of EGFR on the cell membrane. Specifically, we will use fluorescence based image analysis techniques to determine predominant mechanisms of diffusion for the receptor in the presence of the EGFR ligand (epidermal growth hormone factor (EGF)) and without it. The classic diffusion profiles are already well defined in a previous work published from our lab of similar nature [27]. Scientific works in the recent decades predominantly used MSD characterization in conjunction with SPT technique for diffusion studies [27]. Our approach involves using total internal reflection fluorescence (TIRF) microscopy with a fast camera system and requires analysis of entire image. In this work, we analyze these mechanisms characterizing diffusion profiles for entire cell using IMSD technique.

2.2 Image Mean Square Displacement

The prime analysis method we have used in this work to characterize the lateral diffusion of EGFR is the image mean square displacement (IMSD) method. Similar to particle tracking, the IMSD method results in a value of mean squared displacement providing information into molecular diffusion, flow, directionality of flow, directed motion within in a 2D image using correlation functions. The mechanism of how molecules can move can be determined using diffusion maps which are also produced by iMSD analysis. These types of motion include random diffusion, active transport, transient confinement, anomalous sub diffusion, confined or corralled diffusion and binding-unbinding events (Figure. 3 & 5). The

IMSD technique we use analyzes the whole image without separation of particles (like SPT) and is based on the spatiotemporal image correlation function. [27]

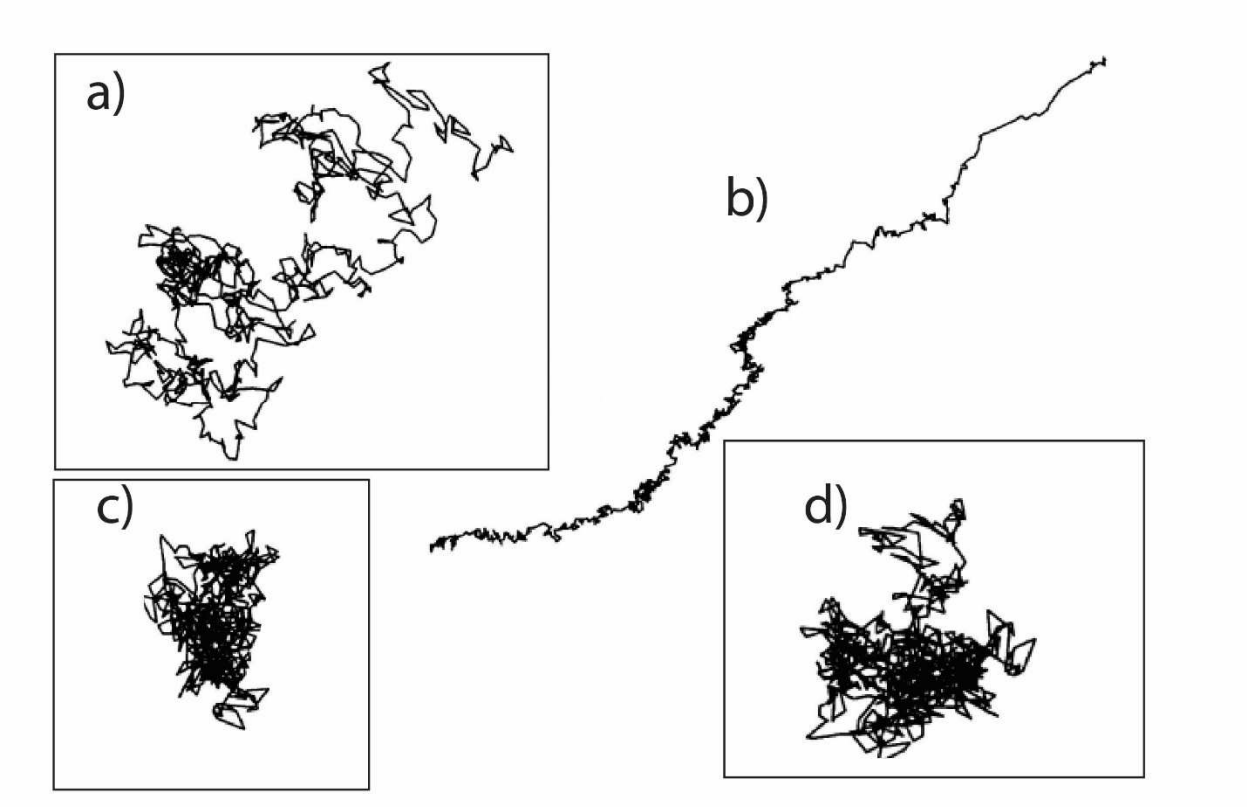

Figure 3: MSD characterizations of four different diffusion profiles a) shows simple or isotropic diffusion mode showing random motion b) shows directed motion c) shows confined diffusion in fixed space d) shows transient confined diffusion curve. [28]

To successfully implement IMSD analysis, it is imperative that we acquire images using 'fast imaging' on the region of interest on the membrane using the TIRF system. This means using a lower exposure time with the camera. The stack of images acquired can then be used to calculate average spatial temporal correlation functions. An apparent diffusivity (D apparent) vs average displacement plot can be acquired by fitting the correlation functions and obtaining the

protein diffusion law. [29] Thus, with the IMSD plot we are able to directly and immediately characterize protein diffusion modes. [30]

The spatio-temporal autocorrelation function can be mathematically expressed as

$$G(\xi,\chi,\tau)=\frac{\langle I(x,y,t)I(x+\xi,y+\chi,t+\tau)\rangle}{\langle I(x,y,t)\rangle}-1$$

Where the measured fluorescence intensity at positions x and y and for a time t is defined as I(x,y,t). ξ is the distance in x and χ is the distance in y while τ represent the time delay. <…> represents the average. In terms of the number of molecules and the autocorrelation of the instrumental waist, this correlation function can be further expressed as

$$G(\xi,\chi,\tau)=\frac{1}{N}p(\xi,\chi,\tau)\otimes W(\xi,\chi)$$

In this expression, N is the number of molecules in the observation volume, $\otimes$ represents the convolution operation. $p(\xi,\chi,\tau)$ is the probability of finding a particle at a distance ξ and χ after a time delay of τ, while $W(\xi,\chi)$ is the autocorrelation of the instrumental waist. Taking into account diffusive dynamics, a Gaussian function can be used to define the probability function, where the variance is the Mean square displacement of the moving particle. $\sigma^2(\tau)$, the waist of the correlation function can be defined as the sum of particle MSDs and the instrumental waist, which can be measured by a Gaussian fitting of correlation function of each

time delay. [29] This enables the calculation of apparent diffusivity and average displacement of the moving molecules:

$$D_{app}(\tau) = \frac{\sigma^2(\tau) - \sigma^2(0)}{4\tau}$$

$$R(\tau) = \sqrt{\sigma^2(\tau) - \sigma^2(0)}$$

Dapp(τ) is the apparent diffusivity of the molecule and R(τ) is the average displacement of the molecule.

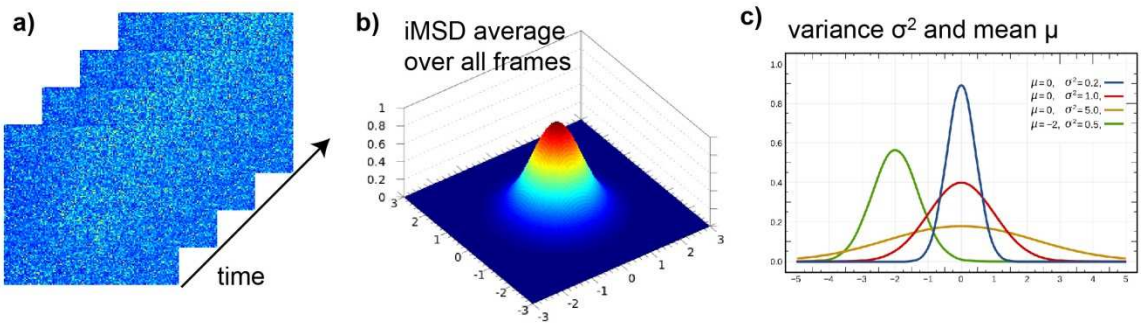

Figure4: a) average image stack acquired to do spatial correlation function. b) 2D Gaussian used to fit the series of correlation functions. c) With the Gaussian, the MSD of the moving particle is the variance, $\sigma^2(\tau)$.

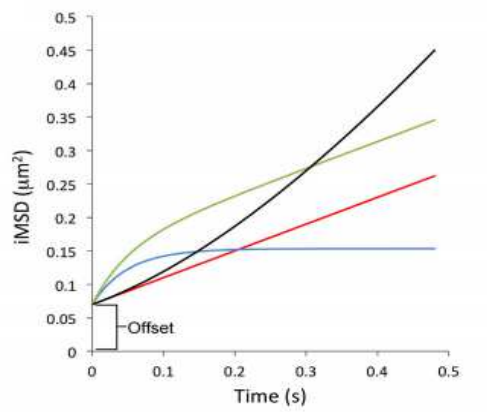

Figure 5: theoretical curves showing all four modes of diffusion, Red represents Brownian motion, Blue is the confined diffusion, black shows directed motion and green is the transient confined mode of diffusion. The intercept at time, t= 0 is the offset due to convolution of the size of the particles and the PSF [27]

The IMSD curves define four modes of diffusion. These diffusion modes can be profiled as isotropic, confined, transiently confined or corralled and directed diffusion or flow. Isotropic diffusion defines random diffusion of molecules, while confined diffusion explains a diffusion profile where the diffusion is confined within the boundaries of a defined space. [28] For transiently confined diffusion, the molecules are able to escape the confinement of the boundary in longer time. The directed diffusion shows a molecule undergoing faster diffusion rates under flow.

2.3 Pair Correlation function

We used the pair correlation analysis technique to understand the molecular flow pattern of the lateral diffusion of the receptor induced by EGF. This analysis method is based on the concept of following the same fluorescent molecule as it diffuses across the membrane. By

following and detecting the same molecule at two different points, average time it takes for the molecule to travel between the points can be calculated. The underlying principle behind this correlation method is that a particle observed at time t= 0 at the origin can be found at a distance r with a probability proportional to the fluorescence intensity at a given distance [31].

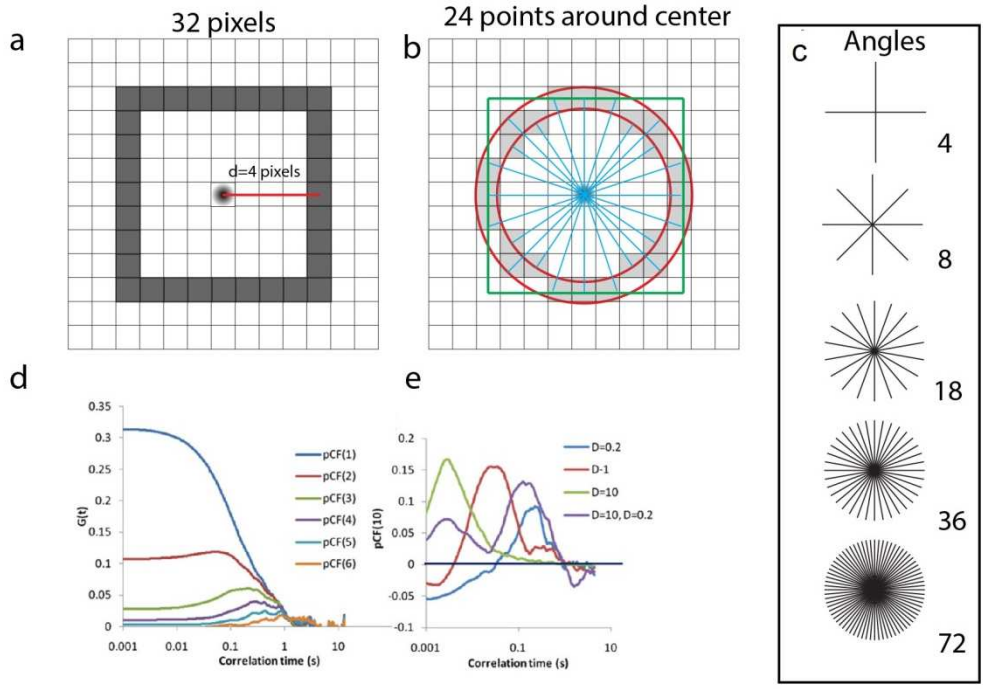

Figure 6: a) Diffusivity for a pCF distance of 4 pixels. b) pCF calculated for 24 points around center at various angles. c) Provision of angles calculated from the point. d,e) pCFs at different PCF distances (from 1 to 6) [left panel] PCF calculated at a distance of 10 pixels for different values of diffusion coefficient, as diffusion coefficient decreases the maximum of pCF function moves at a longer time[31] .

For two points at a distance δr and with a time delay τ, the pCF can be calculated using the following expression

$$G(\tau,\delta r) = \frac{\langle F(t,0)\cdot F(t+\tau,\delta r)\rangle}{\langle F(t,0)\rangle\langle F(t,\delta r)\rangle} - 1.$$

Where the fluorescence intensity at any time and distance δr from the origin can be expressed using the following equation

$$F(t, \delta r) = \kappa Q \int W(r) C(r + \delta r, t) dr,$$

Where Q defines the quantum yield and W(r) is used to define the excitation-emission laser power, filter combination and the position of the particle in the profile of illumination. C(r,t) is the diffusion propagator which is proportional to the probability of finding a particle at position r and time t if the particle is at position r = 0 and time t =0. Mathematically, C(r,t) can be defined as

$$C(r, t) = \frac{1}{(4\pi Dt)^{3/2}} \exp\left(-\frac{r^2}{4Dt}\right)$$

The added benefit of the pCF approach is that it will also enable us to infer any barriers to diffusion along our diffusion pathway. This is accomplished by seeing when the maximum of the pCF occurs. The maximum of pCF at a longer time is attributed to the particle attempting to pass around or over the barrier. The location and size of these obstacles/barriers can be found by mapping the time of maximum of the pCF for every pair of points in the image. [31]

2.4 Number and Brightness

EGFR is activated upon addition of EGF; this activation is characterized by dimerization or higher order oligomerization of the receptor which predominantly exists in monomeric form prior to activation. To verify this activation of the receptor, we use Number and Brightness

(N&B) method which is an analysis method widely used to characterize molecules into different oligomerization forms.

The N&B method was developed as a means to quantify aggregation of molecules, which is a marker for many cellular functions. The number and brightness is determined by the first and second moments of the fluorescence intensity distribution. [32] For a camera based system, such as TIRF, the exposure time of the system determines the time each pixel is sampled for. Thus, with a long enough exposure time, number fluctuations occurring due to fast processes are averaged out while only fluctuations due to slower processes remain. [32]

Mathematically, the parameters apparent brightness (B) and apparent number of particles can be defined as follows.

$$B = \frac{\sigma^2}{< k >}$$

Where B is defined as the ratio of variance to average intensity

$$N = \frac{< k >^2}{\sigma^2}$$

And N is defined as the ratio of total intensity to B. The calculated apparent brightness, B from the variance in intensity fluctuations can then be used to find the true molecular brightness, which is represented by ε in the following equation.

$$B = \epsilon + 1$$

$$\in = \frac{\sigma^2 - < k >}{< k >}$$

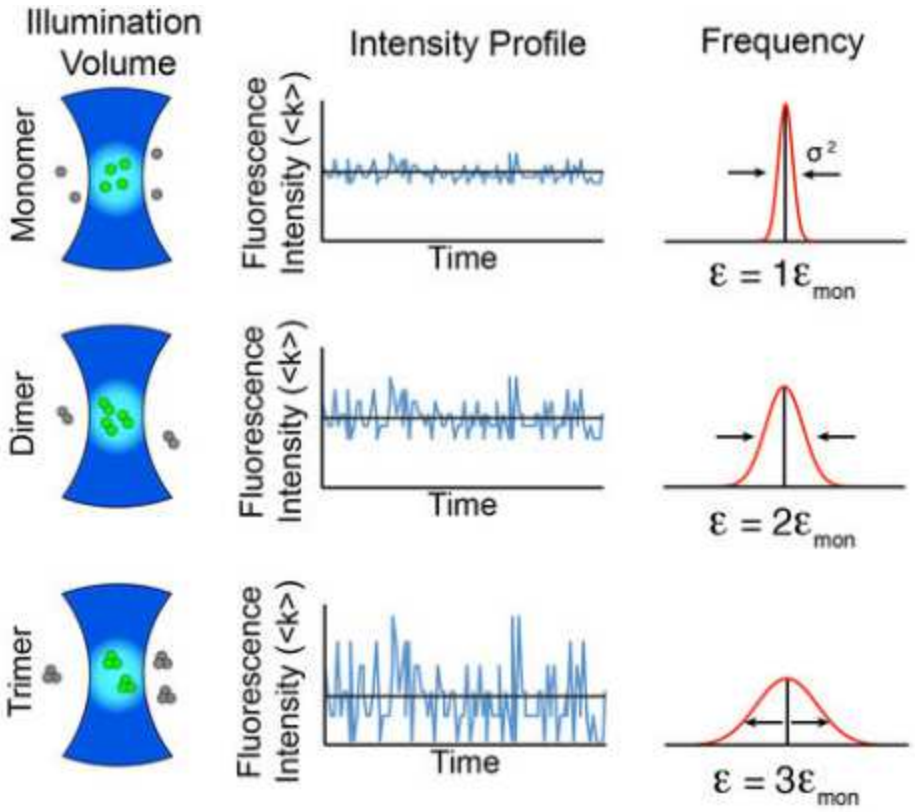

Figure 7: Monomers, dimers and trimers for a PSF is shown. The fluctuation intensities vary for different state, from the fluctuation in intensity, the variance can be obtained, which is related to the aggregative state and can be used to find the apparent brightness B. [33]

When applying this analysis method to biological systems, B represents the aggregates of fluorophore containing molecules and N gives the average number of molecules in the illumination volume [32]. Thus using this analysis method we can confirm and visualize EGFR being activated after addition of EGF, which possibly leads to different diffusive pathways which can be analyzed using other analysis methods discussed in previous sections.

Chapter 3: Methods and Materials

TIRF microscopy:

The principle behind total internal reflection fluorescence (TIRF) microscopy works by ensuring that there is reflection caused by the incident angle, Θi from the excitation light passing through the glass coverslip and interfacing with the sample, being greater than the critical angle, Θc defined by Snell's law.

$$\theta_c = \sin^{-1}(n_1 / n_2)$$

, where n_1 and n_2 are the refractive indices of the sample and the coverslip, respectively. For Total internal refection to occur, the refractive index n1 of the sample need to be less than the refractive index n2 of the coverslip (Figure. 8). [34]

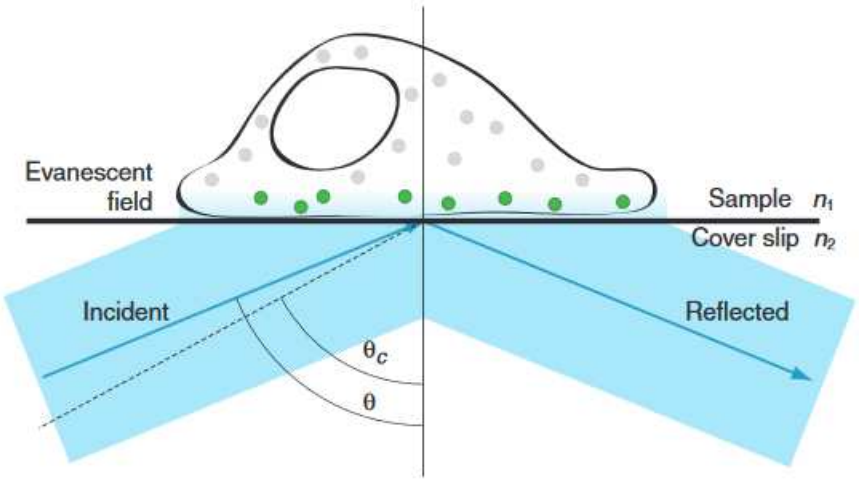

Figure 8: The illustration shows the TIRF principle, where an evanescent field is created as the incident angle is higher than the critical angle and the refractive index, n1 of the sample is less than that of the cover slip, n2. The green dots indicate only the fluorophores that are illuminated under the evanescent field [25]

As stated previously, when the incident angle Θi is greater than the critical angle Θc, the excitation light is reflected off the coverslip interface. When, this occurs, the incident light penetrates through the interface and creates an evanescent field. [34]

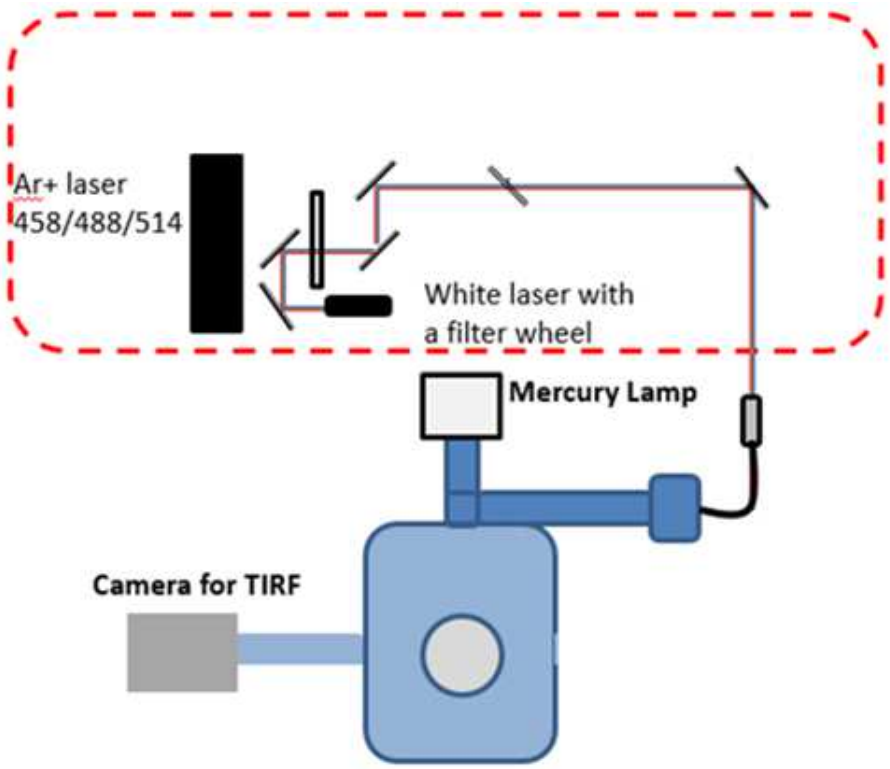

Figure 9: The schematic shows the TIRF setup used for the experiments: two lasers were used for two color excitation, the TIRF camera is attached to an Olympus microscope.

For our study we focused on the cell membrane where EGFR is localized using the TIRF microscope. With the TIRF system, the evanescent wave propagates approximately 100nm inside the cell, which makes it a particularly useful tool in gathering membrane dynamics data. The advantages of TIRF include, obtaining high contrast images of fluorophore near the plasma membrane, very low background from the bulk of the cell, reduced cellular photo damage allowing high signal to noise ratio and rapid exposure times. [34] TIRF minimizes out of focus

intracellular fluorescence, allowing for greater signal to noise ratio and allows the greatest amount of information on the fluorophores associated with the membrane. [34]

The system set up we used for the purposes of the experiments had a two laser system enabling two color excitation, allowing us to capture information in two channels for cross correlating using pair correlation function (pCF). For the purpose of our experiment the FLIM camera was not used, (FLIM Camera is visible in Figure 10 showing actual setup) images were acquired with the EMCCD TIRF camera.

Cell Culturing:

Chinese Hamster Ovary (CHO-K1) cells were cultured at 37%C in media containing Dulbecco's Modified Eagle medium (DMEM)/ F-12 Nutrient mixture supplemented with 10% Fetal Bovine Serum (FBS) and 1% Penstrep at 5% $C0_2$. Transfections were carried out using Lipofectemine 5000 and according to manufactures instructions. After transfections using the EGFR and the monomeric EGFP fused to the membrane targeting sequence GAP-43 plasmid (EGFR-GFP was a gift from Alexander Sorkin (Addgene plasmid # 32751), the cells were plated in imaging dishes and left to grow for 24 hours. For two-color experiments we co-transfected the EGRP plasmid and the Caveolin plasmid (EGFR-GFP was a gift from Ari Helenius; Addgene plasmid #27705) in CHO-k1 cells and performed the same serum starvation prior to adding EGF.

Serum starvation was done four hours prior to imaging. The media in the imaging dish was aspirated and replaced with DMEM F-12 Media without the FBS and the penstrep supplement. This was done to induce greater stimulation by EGF.

TIRF Imaging:

TIRF setup has already been described in chapter 3. Data acquisition was done using 2-color filter by the use of both Fianium white laser and an Argon laser. The cells were transfected with gfp and mcherry plasmids, enabling us to collect data in both the green and red channel. In instances, where the cells were not co-transfected with both fluorophores, data was only collected in one channel appropriate for the transfected plasmid (channel 2 for green and channel 1 for red) using a 256x256 grid; for two color data acquisition a 512x256 grid was used to collect both channels. Images were collected with TIRF EMCCD camera, using a zoon of 2 which corresponds to a pixel size of 0.138 um. The microscope used a 60x oil objective with 1.4 NA. More than 2000 frames were captured at 20k (100ms) exposure time.

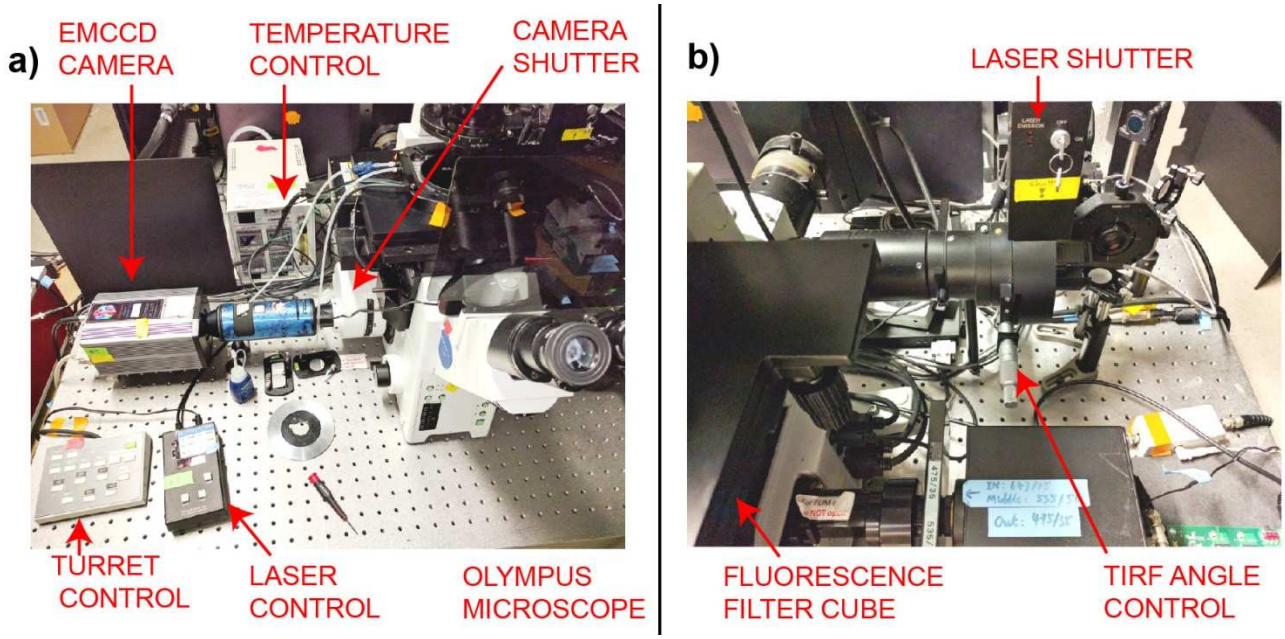

Figure 10: The actual setup of the TIRF system used to acquire data for the purposes of this study. The filter was at position 3 for TIRF mode, Images were first focused using the microscope and then imaged using the TIRF camera.

From the actual setup of the TIRF microscope, the cells were brought in focus, while the camera shutter remained at position S, preventing any light from entering the camera. Once the cells were properly focused, using the computer module, we enable the operation of the camera, the excitation wavelength was selected accordingly, the camera mode was switched on the microscope and the zoom wheel was turned to 2x for imaging (Pixel size= 145nm). Then the laser was turned on and after setting the gain to 4095 in the accompanying software for the camera and selecting the preferred, grid size, we were able to capture images on the camera.

The laser emission shutter is shown in Figure 10, with the on and off mode, turning it on while excite the fluorophores in the imaging dish. One extremely important part of achieving a TIRF image is to ensure that we are at the perfect TIRF angle, adjusting the knob, that changes the fiber optic laser, will allow us to increase or decrease the angle to create the evanescent field, so that we will only see the membrane of the cell. There is also, a filter wheel position can be manually verified on the filter turret wheel on the microscope (the TIRF mode on this microscope is available for filter position 3).

IMSD Analysis: For IMSD analysis, the first step was to ensure that we account for photo-bleaching. Using the intensity of the background signal in our image, the background noise is eliminated. IMSD analysis was done in SimFCS, using all model option, enabling us to distinguish between diffusion profiles. For the analysis, 256 time points were used for the correlation fit using a region of interest of 64 pixels. Immobile fraction was subtracted using the analysis technique. Since, we acquired the data using a zoom of 2 with the TIRF camera, a pixel size of 0.138um was used. A default PSF of 0.3um was used for analysis. For an exposure of 20k, 50 Frames/sec was used to analyze the data under the IMSD function. The correlation function

was calculated after which the IMSD data was processed, the results of which are discussed in the next section.

N&B Analysis: N&B analysis was done using SimFCS. The images acquired from the TIRF microscope was analyzed using the N&B technique with detrend accounting for photo bleaching. For individual images, threshold was set and analysis was done so that the monomer population was centered with a brightness of 1.16. The molecular brightness value was calibrated using cells expressing the membrane bound monomeric eGFP (GAP-eGFP; data not shown). By looking at the population that is above brightness value of 1, we can distinguish between, dimers, trimers and other higher order oligomers. There is a linear relationship between the molecular brightness increase of monomers, dimers and higher order aggregates in such a way that the brightness will increase by 2 fold, 3 fold and so on.

pCF Analysis: In order to detect interaction between caveolin and EGFR, we used the cross-correlation method applied to the pCF analysis. This technique allows us to determine the co-variance of the fluctuations between two labeled species. For our analysis, we measured cross correlating between caveolin-mcherry and the EGFR gfp movement. By doing pCF analysis, we need to ensure that the diffusivity was happening in relation with each other and not independently. In SimFCS, all image pCF analysis was carried to achieve the results for pCF analysis. The analysis was done for a pCF distance of 4, number of angles 26, and 24 number of points around center. Time delay and Eccentricity was plotted, while lower anisotropy threshold was set for 0.1 and upper anisotropy threshold was set for 0.6. A pixel size of 0.138 um was used, and frame time of 0.020 sec. With this analysis we expect to see, cross

correlation in average pCF, illustrated by concentrated red dots in the image after the image is scaled to reduce background noise.

Chapter 4: RESULTS

4.1 IMSD analysis for diffusion profile characterization

Through the IMSD analysis, we analyzed the whole image in an effort to characterize the different diffusion profiles that are prevalent on the cell membrane. After the addition of EGF we will be able to activate the receptor which will dimerize and change the movement of molecules on the cell membrane. This can potentially signal molecular transport to the nucleus. The expectation is to see a marked shift in the overall diffusion profile, before and after the addition of EGF.

According to the work done by Boggara et. al,[11] in characterizing EGFR clusters using single particle tracking, we expect to see a mixture of diffusion profiles with the IMSD analysis on the cell. Their work highlighted, molecules diffusing in primarily three modes: 1) simple diffusion, which we have termed also as isotropic diffusion; 2) confined; 3) and directed diffusion. With the IMSD approach, we also observed transient diffusion as well as the three other diffusion states as mentioned above (Figure.11). However, characterization of molecular motion after the addition of EGF was not studied in living cells. Our measurements are the first to show the changes in diffusion profiles after activation of the receptor. These changes have been theorized biologically but as yet, we have not conclusively proven with an imaging technique.

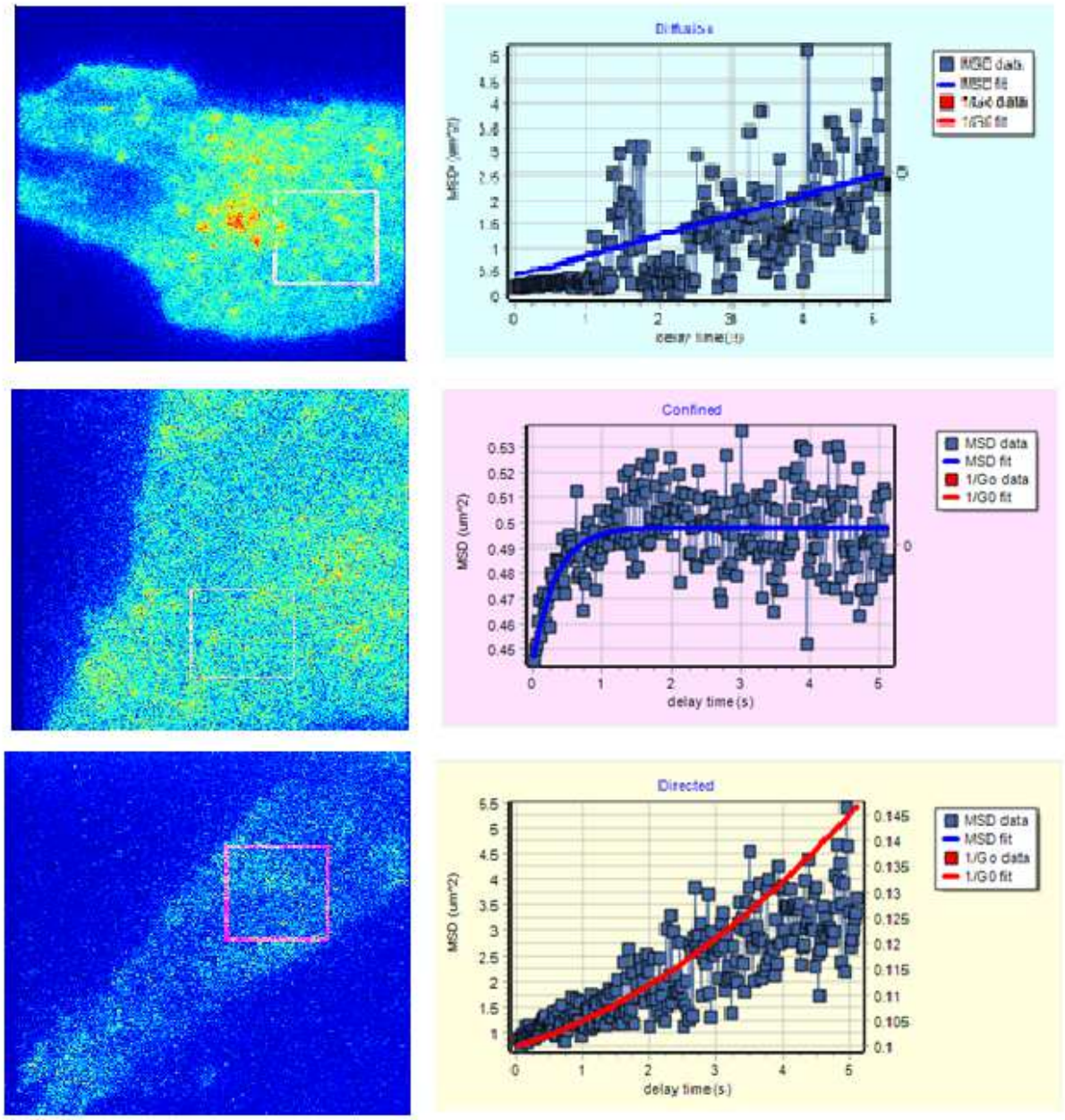

Figure 11: The images above are acquired for individual cells, intended to show varying diffusion profiles for specific regions of interest. We observe all four diffusion profiles on the cell membrane for different regions of interest. The acquisition of data is done according to the method described in the materials and methods section under the methods section describing the IMSD analysis.

The above images show three of the IMSD diffusion profiles as described in the analysis techniques section. For all three images, a region of interest of 64 was chosen with 256 points

to fit. These images show three modes of lateral diffusion that is common on the membrane for the receptor. With our work, we aim to further characterize these diffusion mechanisms to understand their biological relevance to the overall functionality of the receptor.

The IMSD analysis has provided us with similar diffusion profiles as observed by earlier studies that had looked at diffusion profiles of EGFR clustering on the cell membrane. In addition to the three modes of diffusion that has been laid out by Boggara et. al, [11] we have also been able to observed corralled diffusion with our IMSD approach. All four diffusion mechanisms that are described by the IMSD model were observed in our work for characterizing EGFR diffusion on cell membrane.

Below, the data is shown for individual cells after running IMSD analysis on data sets that underwent stimulation by EGF and dataset that is presented before any stimulation. IMSD analysis done for individual images is shown in Figure 12 and 13, the pie chart shows the shift in diffusion profiles for individual cells as influenced by addition of EGF.

Before Addition of EGF

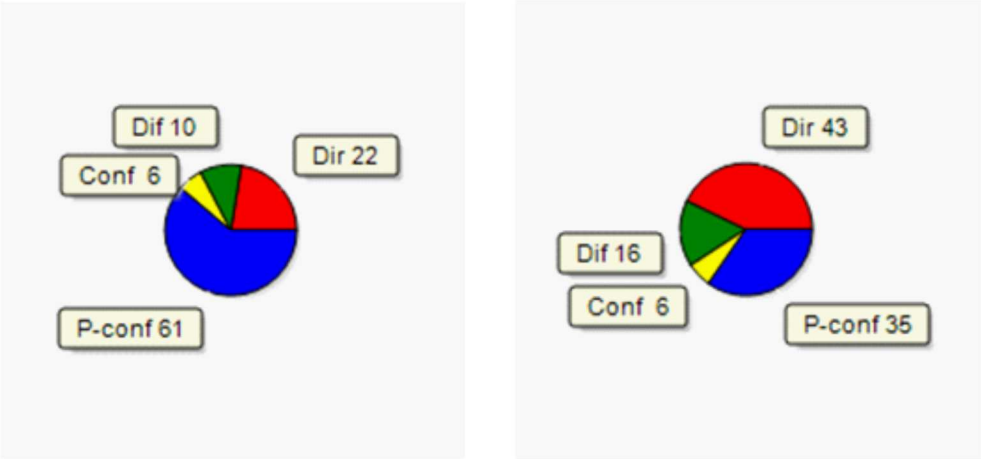

Figure 12: The above pie chart shows the percent distribution of four different diffusion profiles before addition of EGF. Each pie chart is a representation of an IMSD analysis done on two separate cells

Here, we see the diffusion profiles of individual cells, before addition of EGF. All diffusion mechanisms as laid out by the IMSD curves are observed on the cell membrane. For these individual cells shown in Figure 12 the predominant mechanisms are P-conf, which is the transient confined diffusion equivalent in the pie chart, and directed diffusion.

After the Addition of EGF

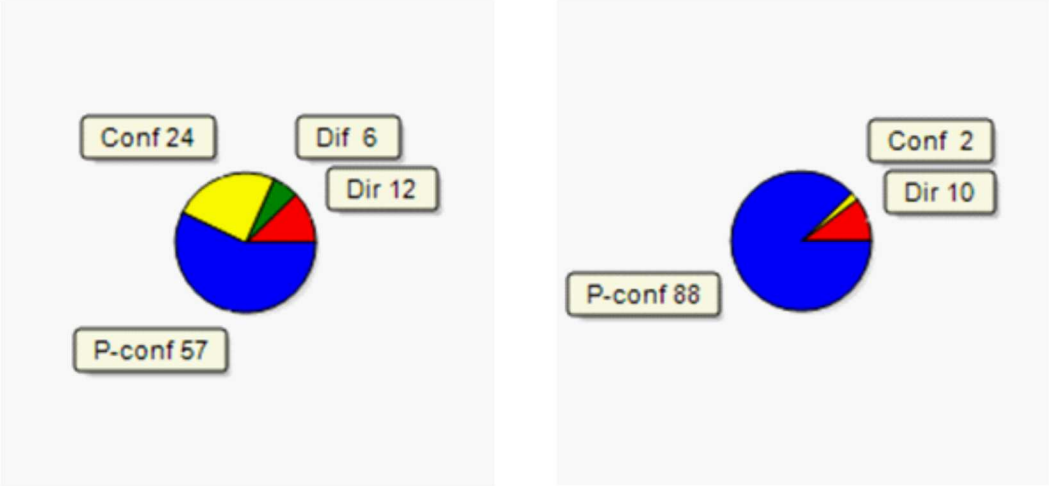

Figure 13: The above pie chart shows the percent distribution of four different diffusion profiles after addition of EGF. Each pie chart is a representation of an IMSD analysis on two separate cells

In Figure 13, we see the breakdown of diffusion profiles, after addition of EGF. For the individual images, the corralled diffusion still remains the predominant diffusion mechanism, even after the addition of EGF. The other two parameters of note are the increase in the confined mode of diffusion. The other striking result after addition of EGF, is that the contribution of directed diffusion is less than before the addition of EGF.

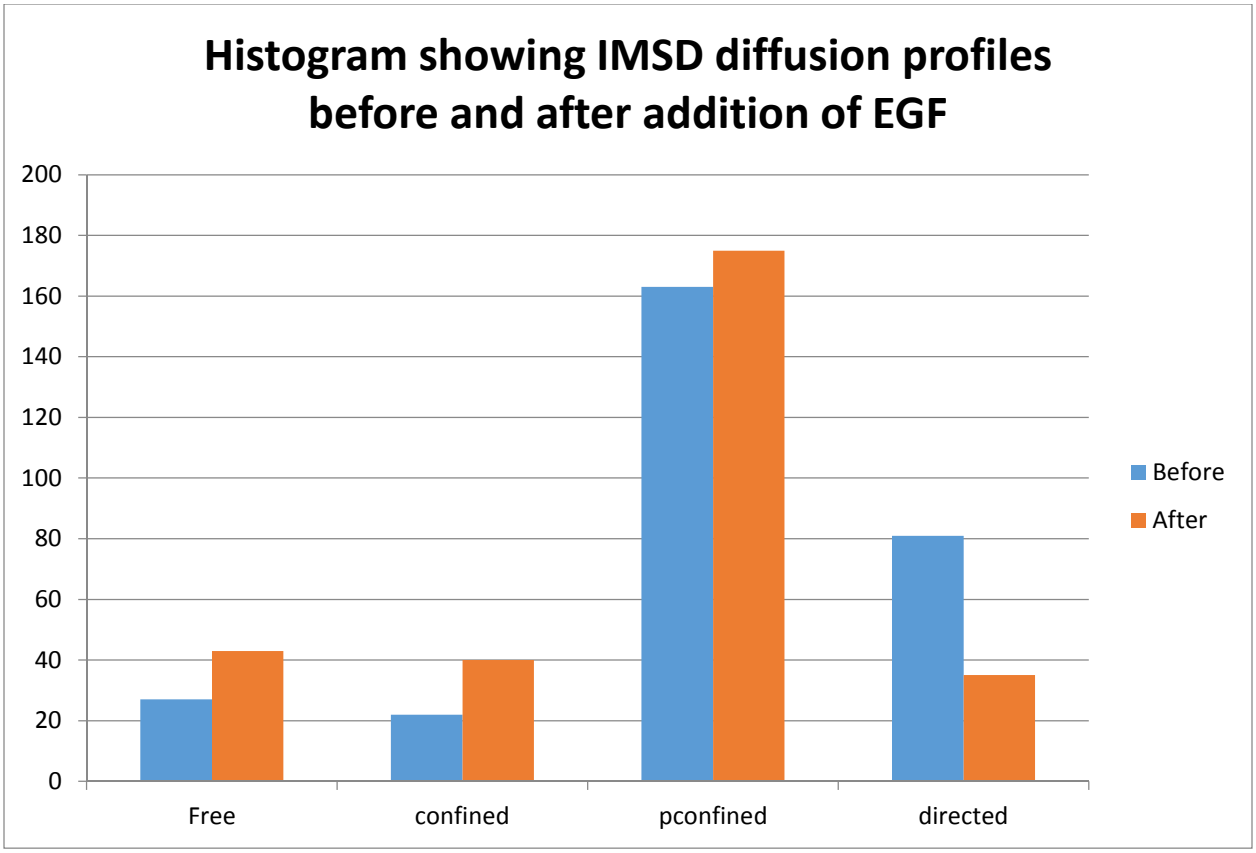

Figure 14: Histogram of diffusion profiles from IMSD analysis of 18 files, y-axis shows the frequency

The IMSD analysis provides an estimate of diffusion profile by plotting the change in MSD over time for multiple segmented regions in the image. The histogram of these profiles from 18 different cells (9 after EGF, 9 before EGF) is plotted in the figure. A custom Student's T test was done on the sorted distribution, which simulated a one tailed heteroscedastic model with before addition of EGF and after addition of EGF as two independent populations. The p-value obtained from the statistical analysis is 0.00168, showing a significant difference in the two datasets. This value does not reflect the statistics of the fitting used or the number of data points, but shows the distribution of profiles are different for the samples with and without EGF. The chart shows that the predominant diffusion mechanisms driving the diffusion on cell

membrane before any stimulation are transient confinement model. Directed diffusion is the second highest contributor, indicating that there is a flow pattern on the cell membrane, regardless of any stimulation

Our predominant aim in doing this work was to observe and characterize the shift in diffusion profiles upon addition of EGF and activation of the receptor. The two striking comparisons are the contributions of transient confinement and confinement models to the overall diffusion profile. Both these confined diffusion profiles increase upon addition of EGF to the cells. The random diffusion mechanism also increases. The other interesting observation from our experiments is the decrease in directed diffusion model.

Looking at the direct comparisons between the diffusion profiles before and after stimulation by EGF of the receptors, we can see that the results point to dominant mechanism of diffusion profile in the cells we imaged as transiently confinement model. Even though after addition there is an increase in the already dominant transient diffusive mechanism, the highest increase in diffusive mechanism is the confinement model post stimulation. The confinement model is almost doubled in terms of overall contribution to diffusivity. The decrease in directed diffusion is also striking, the flow model of diffusion is significantly reduced and the diffusion is predominantly concentrated in confined models, possibly demonstrating the localization and activation of the receptor around caveolar invaginations.

4.2 N&B analysis for analyzing clustering post activation

The number and molecular brightness analysis was used to understand the aggregation process of EGFR in the presence and absence of EGF.

BEFORE EGF

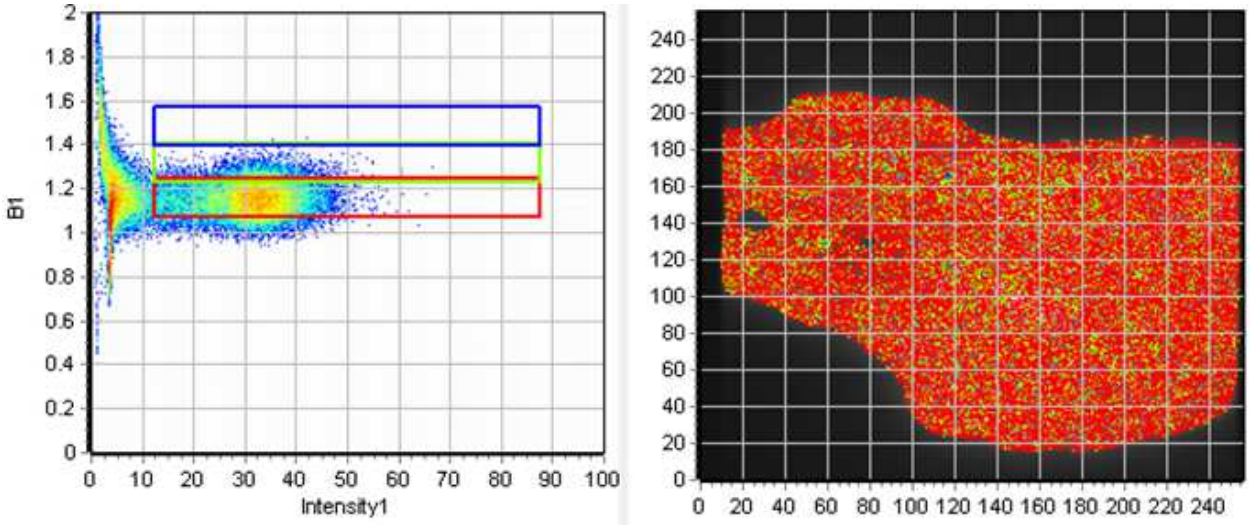

Figure 15: The above illustration is provided to show a N&B analysis carried out on an individual cell before the addition of EGF. The red color overlaying the cell indicates the monomeric population with a molecular brightness equal to 1.16 (ε=0.16 counts/pixel dwell time/molecule) and the green color overlaying the cell indicates the dimeric population for this individual cell, B= 1.32 (ε=0.32 counts/pixel dwell time/molecule).

The Figure15 depicts the results of an N&B analysis done in SIMFCS. The image shows a cell that is being imaged before being stimulated by EGF. The pixels highlighted in red shows monomers in the cell and the green coloring of the pixels are the representation of dimeric aggregates in the cell. The image shows that amount of monomers in the cell highly outweigh the existence of dimers for this particular cell.

AFTER EGF

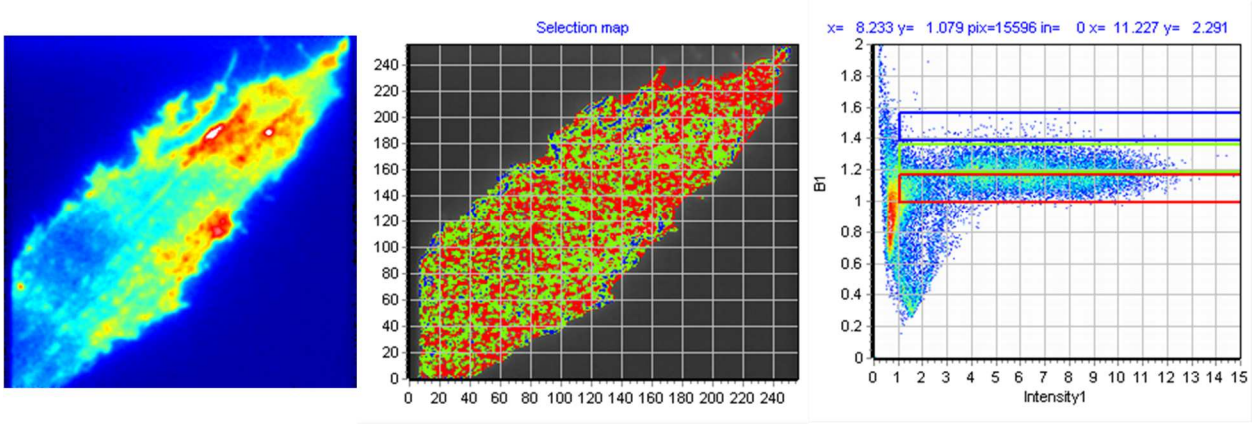

Figure 16: The above illustration is provided to show a N&B analysis carried out on an individual cell after the addition of EGF. The right panel is the average intensity map of the CHO k1 cell expressing EGFR. The middle panel is the molecular brightness map of the protein after the addition of EGF. The red color overlaying the cell indicates the monomeric population and the green color overlaying the cell indicates the dimer population for this individual cell. The last panel is the distribution of molecular brightness using the color cursors mapped in the middle panel.

The Figure16 shows the results of N&B analysis done on a cell that has been stimulated by EGF. As can be seen from the graph, the noise/background level is set to 1 and the monomer population can be found at 1.16. The higher order oligomers, exist as dimers; N&B analysis gives a value of 1.32, approximately two times the value of difference in B1. The monomeric/dimeric map of the cell also shows the increase of dimeric population in the cell, after addition of EGF. The difference is much more apparent when comparing Figure15 and Figure 16, as the monomer: higher order ratio is much higher before stimulating by EGF. The increase of dimeric population after stimulation by EGF is apparent on comparison between the two cells shown in Figures 15 and 16.

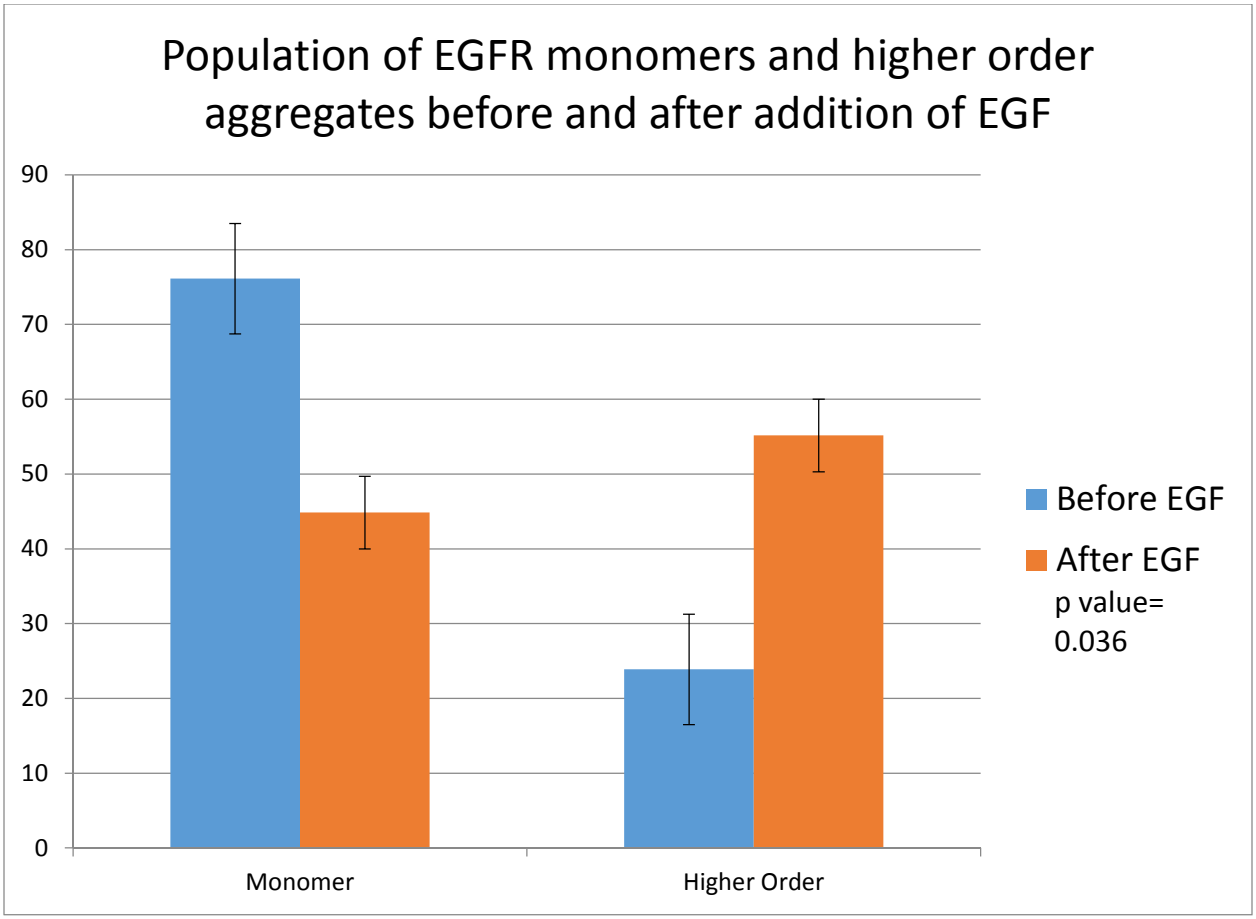

Figure 17: Histogram showing the difference in monomer and higher order aggregates prior to adding EGF and after adding EGF

The graph characterizes the population of molecules in all the cells imaged with TIRF into monomer and higher order aggregates. Analysis was done on approximately 200,000 pixels to characterize the effect of stimulation on clustering and aggregation of particles. A student's T test was done on the distribution shown in Figure 17, using one tailed independent, heteroscedastic model, between populations before addition of EGF and after addition of EGF. The p-value for the test was .036 between the two sets of data. The graph shows an increase in the higher order aggregates after stimulation as well as the monomeric population decreasing

as a result of the activation of the receptor. The monomeric population decreased by approximately 32%. Our analysis shows a very strong mechanism for the activation of EGFR.

4.3 Cross-pCF for cav-EGFR diffusivity

For the investigation of correlated movement of EGFR with caveolin on the cell membrane, we analyze the data using pCF image cross correlation to observe for diffusion mechanisms. pCF here shows the delay in time for a molecule to correlate at a distance of 500nm away from it and the anisotropic nature of this movement from that pixel known as the eccentricity. A high amplitude in time delay shows that the molecule diffused away from the pixel 500 nm away in a longer period of time (4x138nm). Similarly, we can also calculate the eccentricity value 0 (isotropic) to 1 (linear movement) from the occurrences of positive correlations in any given direction. The pCF analysis also shows the direction of movement and the velocity of movement (which are not shown here). The time delay and eccentricity for caveolin channel and the EGFR channel are calculated separately and finally a cross correlation pCF is plotted to identify the cross-correlated movement of both molecules. A complete histogram of time delay of from the image is also plotted together with the pCF images to show the relative speed of motion of cav, EGFR and combined.

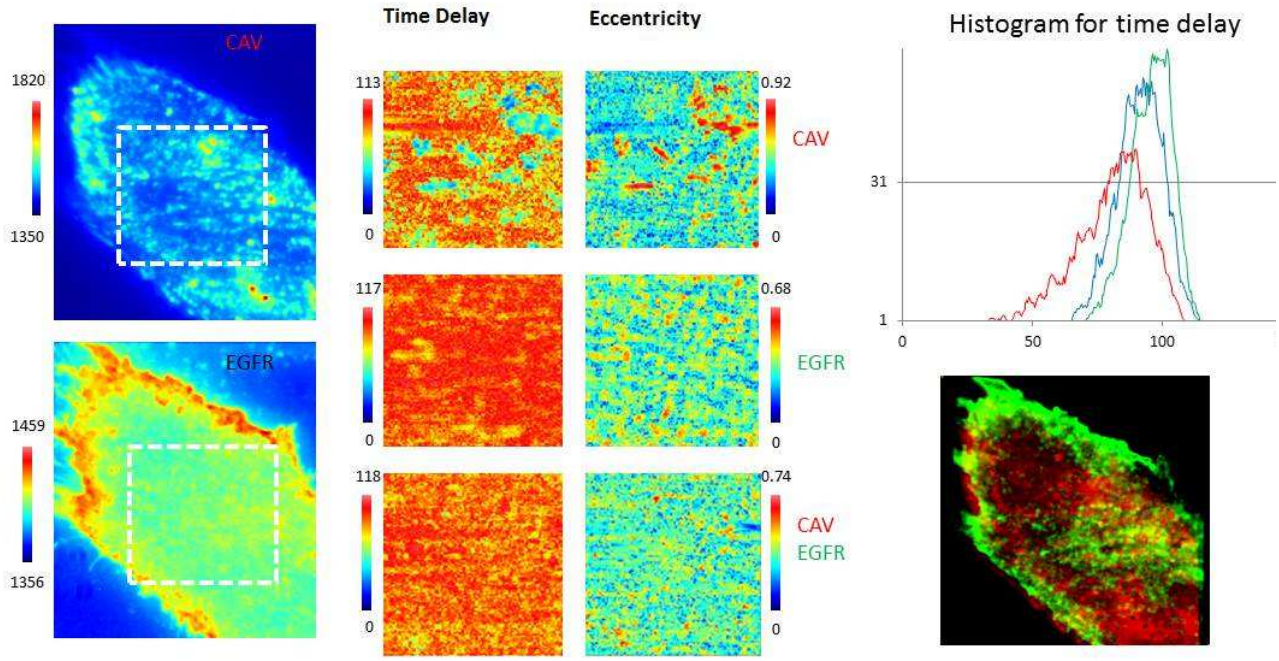

Figure 18: pCF analysis showing time delay maps and eccentricity for a single cell

The time delay map of one pixel shows the time spent by the fluorescent molecule to reach 4 pixels away from that pixel. Reading the sheer magnitude presented in the time delay map, EGFR takes the longest time to reach 4 pixels far from it and caveolin takes shorter time (This is also illustrated in the time delay histogram). The cross correlated time delay image shows only the pixels which correlated and presented a time delay. These pixels showed a time delay shorter than egfr and longer than caveolin, as we may expect from the average diffusion from cav-egfr complex. The eccentricity map (0-1) shows that the caveolin movement has relatively higher anisotropic nature while egfr and correlated cav-egfr shows relatively less anisotropic diffusion inside the cell (quasi-uniform color scale).

CHAPTER 5: DISCUSSION

The IMSD analysis was used to analyze and characterize the different kinds of diffusion profiles that are prevalent on the cell membrane with respect to EGFR. The approach defines four types of diffusion patterns that exist. [27-18] Our aim was to determine if these diffusion patterns are influenced by the stimulation of the cells with epidermal growth factor. From the results of the IMSD analysis, we can see the predominant mechanism for diffusion is explained by the transient confined model. We hypothesized that the receptor should diffuse in a confined model as EGFR is known to localize around caveolin invaginations on and near the cell membrane.[18] Our experiments, show that transient confined mode is the most prevalent mode of diffusion before and after addition of EGF. The increase in the mode of confined diffusion after the addition of EGF, strongly indicates that the receptors are highly localized within the invaginations. Another theory for diffusion for EGFR clusters is that they will move out of the caveolae. However our results indicate a strong localization instead. This localization within the caveolae for EGFR is known to help against degradation and mutation of the receptor and also enables intracellular EGFR signaling.

The Number and Brightness analysis was used to confirm the activation of the epidermal growth factor receptors by mapping the dimer formation after adding EGF. Existing literature points to formation of higher order oligomers, primarily dimers, as an indication of activation of the EGFR, and beginning of signaling modules that are important to various cell functions. [6-7] With our N&B approach we can confirm and validate this apparent activation of the receptor upon addition of the cells in the imaging dish by epidermal growth factor (EGF). There is a

significant increase in dimeric population once the cells are stimulated by the EGF (~32% of the population, overall). The predominant mechanism that has been shown as an activator is the dimerization of the receptor, even though, higher order oligomers are known to exist.

PCF allows one to visualize pixel to pixel cross correlation, which is an arduous and rigorous computational method compared iMSD. With pCF analysis presented in this thesis, we are able to show that caveolin and EGFR cross correlated movement can be visualized. Furthermore, we presented the time delay map which illustrated that the cross correlated movement of egfr-cav takes longer time than egfr movement. Similarly, the eccentricity map presented shows that the movement of cav is relatively anisotropic compared to cav-egfr complex. We believe that this caveolin eccentricity maps shine new light into the unseen barriers for membrane diffusion and organization.

CHAPTER 6: CONCLUSIONS AND FUTURE DIRECTIONS

6.1 CONCLUSIONS

Our experiments were beneficial in two regards. Firstly, they helped solidify our understanding of biological behaviors that is demonstrated by Epidermal Growth Factor Receptor. Secondly, we had to prove that the techniques we use can characterize diffusion profiles. We use these methods to reinforce our understanding of EGFR behavior in response to EGF. We further characterize this behavior with parameters such as the diffusion profile exhibited by the receptor. Diffusion profiles served as a parameter that needs understanding in the existing biological framework of EGFR behavior. N&B approach has already been proven as a valid method of analysis of clustering and aggregation of molecules. The aggregates that formed upon the activation of the receptor were in accordance with what we already knew biologically about the receptors after EGF stimulation. This further reinforces the validity of our methods.

While many studies have tried to characterize the diffusion of the EGFR, the commonly used technique is the single particle tracking method. In looking at protein interactions, this is a limited approach, especially when studying rapid phenomena for large numbers. IMSD provides the added benefit of analyzing the whole image to understand receptor activity at a cellular level. IMSD was our predominant analytical tool in understanding the receptor activity as it clearly characterized the predominant diffusion mechanisms which goes hand in hand with our understanding of caveolin-EGFR interactions. The localization of the EGFR clusters around the

invaginations are well studied and we believe the transient confinement and confinement model that we observe here defines the activity as such, that it is possible that after activation and clustering, the receptor localizes more in the caveolin invagination before starting the signaling process indicating cytoplasmic transport. This is a known mechanism that our IMSD approach verifies at the cell membrane level.

6.2 FUTURE DIRECTIONS

As described earlier, EGFR receptor activity is highly varied along different cell types. As such, it would be important to characterize EGFR behavior upon activation with multiple cell lines. With the IMSD approach, we hope to further find threads between different cell lines that have previously not been discovered. We have other parameters that are of interest that might help us in the future to understand the behavior of the receptor, such as cell shape and temperature. Varying these parameters and repeating our study might be a worthwhile attempt to yet again show the powerful technique of IMSD.

With IMSD technique, we enabled analyzing diffusion profiles across the cells in various regions of interest. Ideally, we want to do a pixel resolution diffusion map for a more comprehensive study. For this purpose, in the future, we would like to analyze our test data with diffusion phasors. This method gives us a detailed diffusion map inside the cell by plotting the diffusion profile with pixel resolution in fourier space. To date, this diffusion phasor has been done with a scanning setup, nevertheless our future work would entail the first instance of where this method is employed in conjunction with a camera based system. In this approach, slow diffusion is characterized by larger phase angles and fast diffusion is represented by

smaller phase angles. Thus this method will enable us to map out areas on the cell membrane that exhibits different diffusion velocities and characterize the impact of EGFR activation with a new parameters of interest.

REFERENCES

[1] Singer, S.J., and G.L. Nicolson. 1972. The fluid mosaic model of the structure of cell membranes. Science. 175:720–731.

[2] Feigin, Michael E., and Senthil K. Muthuswamy. "ErbB receptors and cell polarity: new pathways and paradigms for understanding cell migration and invasion." *Experimental cell research* 315.4 (2009): 707-716

[3] Marmor, Mina D., Kochupurakkal Bose Skaria, and Yosef Yarden. "Signal transduction and oncogenesis by ErbB/HER receptors." *International Journal of Radiation Oncology* Biology* Physics* 58.3 (2004): 903-913.

[4] Yarden, Yosef, and Mark X. Sliwkowski. "Untangling the ErbB signalling network." *Nature reviews Molecular cell biology* 2.2 (2001): 127-137.

[5] Lemmon, Mark A. "Ligand-induced ErbB receptor dimerization." *Experimental cell research* 315.4 (2009): 638-648.

[6] Clayton, Andrew HA, et al. "Ligand-induced dimer-tetramer transition during the activation of the cell surface epidermal growth factor receptor-A multidimensional microscopy analysis." *Journal of Biological Chemistry* 280.34 (2005): 30392-30399.

[7] Nagy, Peter, et al. "Distribution of resting and ligand-bound ErbB1 and ErbB2 receptor tyrosine kinases in living cells using number and brightness analysis." *Proceedings of the National Academy of Sciences* 107.38 (2010): 16524-16529.

[8] Wiegant, F. A., et al. "Epidermal growth factor receptors associated to cytoskeletal elements of epidermoid carcinoma (A431) cells." *The Journal of cell biology* 103.1 (1986): 87-94.

[9] Den Hartigh, Jan C., et al. "The EGF receptor is an actin-binding protein." *The Journal of Cell Biology* 119.2 (1992): 349-355.

[10] Lidke, Diane S., et al. "Reaching out for signals filopodia sense EGF and respond by directed retrograde transport of activated receptors." *The Journal of cell biology* 170.4 (2005): 619-626.

[11] Boggara, Mohan, et al. "Characterization of the diffusion of epidermal growth factor receptor clusters by single particle tracking." *Biochimica et Biophysica Acta (BBA)-Biomembranes* 1828.2 (2013): 419-426.

[12] Abulrob, Abedelnasser, et al. "Nanoscale imaging of epidermal growth factor receptor clustering effects of inhibitors." *Journal of Biological Chemistry* 285.5 (2010): 3145-3156.

[13] Cordes, N., et al. "Human pancreatic tumor cells are sensitized to ionizing radiation by knockdown of caveolin-1." *Oncogene* 26.48 (2007): 6851-6862.

[14] Tanos, Barbara, and Ann Marie Pendergast. "Abl tyrosine kinase regulates endocytosis of the epidermal growth factor receptor." *Journal of Biological Chemistry* 281.43 (2006): 32714-32723.

[15] Wanner, Gabriele, et al. "Activation of protein kinase Cε stimulates DNA-repair via epidermal growth factor receptor nuclear accumulation." *Radiotherapy and Oncology* 86.3 (2008): 383-390.

[16] Dittmann, Klaus, et al. "The radioprotector O-phospho-tyrosine stimulates DNA-repair via epidermal growth factor receptor-and DNA-dependent kinase phosphorylation." *Radiotherapy and Oncology* 84.3 (2007): 328-334.

[17] Ushio-Fukai, Masuko, and R. Wayne Alexander. "Caveolin-dependent angiotensin II type 1 receptor signaling in vascular smooth muscle."*Hypertension* 48.5 (2006): 797-803.

[18] Abulrob, Abedelnasser, et al. "Interactions of EGFR and caveolin-1 in human glioblastoma cells: evidence that tyrosine phosphorylation regulates EGFR association with caveolae." *Oncogene* 23.41 (2004): 6967-6979.

[19] Mills, Ian G. "The interplay between clathrin-coated vesicles and cell signalling." *Seminars in cell & developmental biology*. Vol. 18. No. 4. Academic Press, 2007.

[20] Mineo, Chieko, Gordon N. Gill, and Richard GW Anderson. "Regulated migration of epidermal growth factor receptor from caveolae." *Journal of Biological Chemistry* 274.43 (1999): 30636-30643.

[21] Rodemann, H. Peter, Klaus Dittmann, and Mahmoud Toulany. "Radiation-induced EGFR-signaling and control of DNA-damage repair." *International journal of radiation biology* 83.11-12 (2007): 781-791.

[22] Saito, Tsugumichi, et al. "Differential activation of epidermal growth factor (EGF) receptor downstream signaling pathways by betacellulin and EGF." *Endocrinology* 145.9 (2004): 4232-4243.

[23] Drube, Sebastian, et al. "Ligand-independent and EGF receptor-supported transactivation: Lessons from β2-adrenergic receptor signalling." *Cellular signalling* 18.10 (2006): 1633-1646.

[24] Chung, Inhee, et al. "Spatial control of EGF receptor activation by reversible dimerization on living cells." *Nature* 464.7289 (2010): 783-787.

[25] Valley, Christopher C., Keith A. Lidke, and Diane S. Lidke. "The spatiotemporal organization of ErbB receptors: insights from microscopy." *Cold Spring Harbor perspectives in biology* (2013): a020735.

[26] Di Rienzo, Carmine, et al. "Fast Spatiotemporal Correlation Spectroscopy to Determine Protein Lateral Diffusion Laws in Live Cell Membranes." *Biophysical Journal* 106.2 (2014): 224a.

[27] Moens, Pierre DJ, Michelle A. Digman, and Enrico Gratton. "Modes of diffusion of cholera toxin bound to GM1 on live cell membrane by image mean square displacement analysis." *Biophysical journal* 108.6 (2015): 1448-1458.

[28] Kusumi, Akihiro, Yasushi Sako, and Mutsuya Yamamoto. "Confined lateral diffusion of membrane receptors as studied by single particle tracking (nanovid microscopy). Effects of calcium-induced differentiation in cultured epithelial cells." *Biophysical journal* 65.5 (1993): 2021.

[29] Di Rienzo, Carmine, et al. "From fast fluorescence imaging to molecular diffusion law on live cell membranes in a commercial microscope." *Journal of visualized experiments: JoVE* 92 (2013): e51994-e51994.

[30] Di Rienzo, Carmine, et al. "Fast Spatiotemporal Correlation Spectroscopy to Determine Protein Lateral Diffusion Laws in Live Cell Membranes." *Biophysical Journal* 106.2 (2014): 224a.

[31] Digman, Michelle A., and Enrico Gratton. "Imaging barriers to diffusion by pair correlation functions." *Biophysical journal* 97.2 (2009): 665-673.

[32] Digman, Michelle A. et al. “Mapping the Number of Molecules and Brightness in the Laser Scanning Microscope.” *Biophysical Journal* 94.6 (2008): 2320–2332. *PMC*. Web. 1 May 2016.

[334] Mieruszynski, Stephen, et al. "Live cell characterization of DNA aggregation delivered through lipofection." *Scientific reports* 5 (2015).

[34] Mattheyses, Alexa L., Sanford M. Simon, and Joshua Z. Rappoport. "Imaging with total internal reflection fluorescence microscopy for the cell biologist." *Journal of cell science* 123.21 (2010): 3621-3628.